Engineering Geology 128 (2012) 63–75

Contents lists available at ScienceDirect

Engineering Geology

journal homepage: www.elsevier.com/locate/enggeo

Analysis of debris flow behavior with a one dimensional run-out model incorporating entrainment

B. Quan Luna [a,*], A. Remaître [b], Th.W.J. van Asch [c], J.-P. Malet [b], C.J. van Westen [a]

[a] United Nations University-ITC School for Disaster Geo-information Management, University of Twente, Enschede, The Netherlands
[b] Institut de Physique du Globe de Strasbourg - IPGS, CNRS & Université de Strasbourg, Strasbourg, France
[c] Utrecht University, Faculty of Geosciences, Utrecht, The Netherlands

ARTICLE INFO

Article history:
Accepted 8 April 2011
Available online 17 April 2011

Keywords:
Debris flows
Run-out
Entrainment
Erosion
Modeling

ABSTRACT

Estimating the magnitude and the intensity of rapid landslides like debris flows is fundamental to evaluate quantitatively the hazard in a specific location. Dynamic run-out models are able to characterize the distribution of the material, its intensity and define the zones where the exposed elements will experience an impact. These models can provide valuable inputs for vulnerability and risk calculations. However, most dynamic run-out models assume a constant volume during the motion of the flow, ignoring the important role of material entrained along its path. Consequently, they neglect that the increase of volume can enhance or reduce the mobility of the flow and can significantly influence the size of the potential impact area.

Limited work has been done to quantify the entrainment process and only a few have proposed physical explanations for it. One of the reasons is that material entrainment is a complex process and an adequate understanding of the phenomenon is needed to facilitate the development of appropriate dynamic models. A proper erosion mechanism needs to be established in the analyses of debris flows that will improve the results of dynamic modeling and consequently the quantitative evaluation of risk.

The objective of this paper is to present and evaluate the performance of a 1D debris flow model with a material entrainment concept based on limit equilibrium considerations and the generation of excess pore water pressure through undrained loading of the in-situ bed material. The debris flow propagation model is based on a one dimensional continuum mechanics approach using a depth-integrated approximation based on the shallow water assumption (Saint–Venant equations). The flow is treated as a laminar one-phase material, in which behavior is controlled by a visco-plastic Coulomb–Bingham rheology. The model parameters are evaluated and the model performance is tested on a debris flow event that occurred in 2003 in the Faucon torrent (Southern French Alps).

1. Introduction

Debris flows play an important role in the sediment transfer and erosion in mountainous areas, and constitute an important risk to the population. Due to their capacity to travel long distances at high velocities, the threats to human life and property from debris flows are greater than those of other landslides types (Begueria et al., 2009). Entrainment of channel path and torrent flanks material, and sediment deposition during run-out are key features of many debris flows. Such entrainment mechanisms are able to change significantly the mobility of the flow, through rapid changes of the flow volume and its rheological behavior (Iverson et al., 1997; McDougall and Hungr, 2005, Takahashi, 2009).

The entrainment process is frequently observed on debris flows during the run-out phase (Chen et al., 2006, Remaître, 2006). After the failure at the source zone, the entrained materials may accumulate several times in volume with respect to the initially mobilized mass (Vandine and Bovis, 2002). Entrainment occurs when a flow moves along an erodible layer applying a shear stress that surpasses the strength of the erodible layer material. This process can occur during short intervals or semi-continuously over large areas. Single particles or larger pieces of the bed material will be detached and accelerated by the flow and frequently added into it (Gauer and Issler, 2004). Entrainment can either accelerate or decelerate the moving mass depending on the characteristics of the erodible material as well as on the topography and on the dynamics of the flow (Mangeney et al., 2010).

In recent times, several dynamic run-out models for debris flows have been developed and applied for hazard evaluation, risk assessments and the design of mitigation measures (Iverson and Denlinger, 2001; Hungr et al., 2005; van Westen et al., 2006). These dynamic models are physically-based and solved numerically, simulating the movement of the flow using constitutive laws of

* Corresponding author at: United Nations University-ITC School for Disaster Geo-information Management, Faculty of Geo-information Science and Earth Observation (ITC), University of Twente, Hengelosestraat 99, P.O Box 6, 7500AA, Enschede, The Netherlands. Tel.: +31 534874416; fax: +31 534874336.
E-mail address: quanluna@itc.nl (B.Q. Luna).

0013-7952/$ – see front matter © 2011 Elsevier B.V. All rights reserved.
doi:10.1016/j.enggeo.2011.04.007

fluid mechanics in one (1-D) or two dimensions (2-D). Most models are based on a "continuum approach" that considers the loose unsorted material and multiphase moving mass of a debris flow as a continuum. A continuum approach enhances the possibility to model the dynamics of debris flows using an "equivalent" fluid, whose rheological properties are such that the bulk behavior of the numerically simulated flowing mass can approximate the expected bulk behavior of the real mixture of the solid and fluid phases (Hungr and McDougall, 2009). Savage and Hutter (1989), developed a continuum mechanical theory (known also as the Savage and Hutter model) capable of describing the evolving geometry of a finite mass of a granular material and the velocity distribution as it slides down an inclined plane (Pudasaini and Hutter, 2007). In the Savage and Hutter model, the mass and momentum are averaged over the depth and a scaling analysis is performed with respect to the aspect ratio of the flowing mass, considered to be small. This allows modeling the flow by a Saint–Venant type system (shallow water equations) derived in a reference frame linked to an inclined plane (Bouchut et al., 2008). The depth-averaged shallow water equation approach using different solvers has been applied commonly for numerical simulations of rapid mass movements over complex topographies (e.g. Chen and Lee, 2000; Iverson and Denlinger, 2001; Pouliquen and Forterre, 2002; Crosta et al., 2003; Mangeney-Castelnau et al., 2005; Pitman and Le, 2005; Pudasaini and Hutter, 2007; Mangeney et al., 2007; Pastor et al., 2009; Hungr and McDougall, 2009; Medina et al., 2008; Begueria et al., 2009; Christen et al., 2010). Depth averaging allows representing the rheology of the flow as a single term that expresses the frictional forces that interact at the interface between the flow and the bed path. The most common rheologies used in the dynamic models are: the "Frictional" (or "Coulomb") resistance (Hungr and McDougall, 2009); the frictional-turbulent "Voellmy" resistance (Voellmy, 1955); the visco-plastic "Bingham" (or "Herschel–Bulkey") resistance (Coussot, 1997; Malet et al., 2004); the "Quadratic" resistance (O'Brien et al., 1993); and the "Pouliquen" flow law (Pouliquen and Forterre, 2002; Mangeney et al., 2007; Pirulli and Mangeney, 2008). A more thorough description of rheologies commonly used for simulating debris flows can be found in Naef et al. (2006), van Asch et al. (2007), and Hungr and McDougall (2009).

Models using both a constant rheology and a constant volume cannot yield accurate forecast of debris flows characteristics especially for debris flows occurring in heterogeneous torrential watersheds characterized by various geological settings and superficial surface deposits (Crosta et al., 2009). Erosion processes affect the motion in two different ways: firstly the addition of mass to the flow causes a decrease in the bed friction force per unit mass and in the potential energy of the flow, and secondly generates a resistive force on the moving mass, because of the momentum transfer between the flow in motion and the soil cover that has to be mobilized and accelerated to the flow velocity. For this reason, the entrainment mechanisms have to be included in the depth-averaged flow models through erosion and deposition rate formulas, and the addition of an entrainment force term in the momentum balance equation (Issler and Johannesson, 2011). However, its parameterization can become a cumbersome task because of an actual poor understanding and limiting assumptions of the physics and mechanics behind the involved processes (Bouchut et al., 2008). This adds to the lack of consistency of depth-averaged models that includes entrainment laws.

In this paper, we describe and present a dynamic depth-averaged 1D debris flow model that takes into account an entrainment concept based on the limit equilibrium theory and the generation of excess pore water pressure through undrained loading of the in-situ material. The flow is treated as a laminar one-phase material, where behavior is controlled by a visco-plastic Coulomb–Bingham rheology. The purpose is to identify and state the advantages of including entrainment in the calculation of practical debris flow dynamics for hazard analysis. First, a sensitivity evaluation of the efficiency and reliability of the model is performed. Second, the model is calibrated on observational data of a debris flow event that occurred in 2003 in the Faucon torrent (Southern French Alps).

2. Entrainment mechanism analysis—brief summary of previous work

Some efforts have already been made to quantify the erosion processes and entrained volumes, trying to propose a physical explanations for the extreme bulking rates (e.g. Takahashi, 1978; McDougall and Hungr, 2005; Crosta et al., 2009; Mangeney et al., 2010). We divide this previous work in: experimental investigations, empirical and numerical analyses.

2.1. Experimental investigations

Experiments to understand the physics and to construct mathematical models for entrainment rates have been performed at laboratory and full scale. In the past, most of the full scale experiments have been carried out with snow avalanches. Sovilla et al. (2006) based on her observations in the Monte Pizzac (Italy) and Vallée de la Sionne (Switzerland) test sites concluded that in spite of the differences of the snow characteristics and released mass, the maximum erosion took place where the slope is 35° or more. The erosion process decreased where the slopes became gentler. The initial mass, the amount of erodible snow and the avalanche velocity were found to be correlated to the erosion per unit area. She recognized three different mechanisms of snow entrainment: ploughing, step entrainment and basal erosion or abrasion. Ploughing or front entrainment rates measurements where as high as 350 kg m^{-2} s^{-1} (in the Vallée de la Sionne test site) and the entire snow cover can be entrained in a very short time. The step entrainment can also lead to high entrainment rates but is less common. It depends on the layered structure of the snow cover. In step entrainment, the abrasive stresses the avalanche applies to the running layer can cause a crust layer to collapse. However, the entrainment location is no longer directly at the front. Basal erosion is the third possible mechanism but entrainment rates due to this process are low. Recently, Iverson et al. (2011) conducted entrainment experiments in a large 95-m-long and 2-m-wide flume in which water saturated debris flows (containing a mixture of 56% of gravel, 37% of sand and 7% mud sized grains) were discharged abruptly across a partially saturated bed. The key variable that was manipulated during the experiments was the bed sediment volumetric water content. Iverson et al. (2011) findings were that entrainment is accompanied by an increased flow momentum and velocity only if large positive pore pressures develop in wet bed sediments as the sediments are overridden by the flows. The increased pore pressures facilitates progressive scour of the bed, reduces basal friction and instigates positive feedback that causes flow velocity, mass and momentum to increase.

Laboratory scale experiments attempts to replicate the entrainment process in a controlled environment. The most common setup is a defined granular mass that flows over an inclined plane that is covered by an erodible layer. Flume tests and a dimensional analysis were conducted to investigate the characteristics of bed erosion by Egashira et al. (2001) and Papa et al. (2004) proposing a formula for erosion-deposition rate. They observed that bed slope is always adjusted to its equilibrium value in case of debris flows over erodible bed. A debris flow either erodes bed material or leaves sediment on the bed from the body so as to form an equilibrium bed slope. The rate is a product of the depth averaged velocity of debris flow body, the sediment concentration in the non-flowing layer by volume, the bed slope and the equilibrium bed slope corresponding to sediment concentration of the debris flow body (mass density of sediment particles, the mass density of water, the depth averaged sediment

concentration of debris flow by volume and the interparticle friction angle of sediment particles). Sediment deposition takes place when the bed slope is less than the equilibrium bed slope resulting in a negative value of erosion rate. Takahashi (2001) performed flume experiments to obtain the erosion and a deposition characteristic of avalanches. The flume bed was set to a longitudinal slope of 35°. The experimental flow compressed and eroded the bed layer. From such an experimental result a model of erosion velocity was proposed relating the thickness of the bed layer, the velocity of the avalanche and the length of the front part of the avalanche. As for the deposition velocity, an experiment was carried out setting the flume gradient to 30°. The velocity near the bed decreased at first; the slip velocity, however, was still high, and the velocity decreased gradually showing the characteristic movement of a rigid body. Therefore, it is possible to assume that the whole flow stops in a short time as soon as the velocity becomes smaller than a threshold value. This was also in agreement with the observations made by Barbolini et al. (2005) in their laboratory experiments. They also observed and agreed with the observations made by Sovilla et al. (2007) that ploughing was the main mechanism responsible for the erosion of the bed material. Abrasion at the surface of separation between the incoming flow and the erodible layer was also observed, but this mechanism was mainly responsible for the inclusion of eroded particles into the moving material. The experiments performed by Mangeney et al. (2010) confirm that the front zone of the flow, the inclination of the slope and the thickness of the bed layer play a key role in the erosion process. They propose a function for granular collapse deposits between the inclination angle of the plane and the friction angle of the material involved. An increase of 40% in the run-out distance was observed on moderate slopes that are close to the response angle of the grains. Their findings are in accordance to the observations of Crosta et al. (2009) and the experiments of Rickenmann et al. (2003), where erosion efficiency increases as the slope increases; and for gentler slopes the flow is insensitive to the presence of an erodible layer or can even reduce the run-out of the flow.

2.2. Empirical analyses

McDougall and Hungr (2005) proposed an empirical rule of erosion velocity related to the growth rate. They defined the growth rate as the bed-normal depth eroded per unit flow and unit displacement. The volume of entrained material grows with the volume of the initial mass and velocity. In this approach the growth rate is already specified and is exponential with travel length of the flow. Chen et al. (2006) proposed a new concept of yield rate based on the assumption that the volume eroded is proportional to the surface area to be affected and the travelled distance of the centre of mass. A correction coefficient is applied to account for the system non-linearity. In a similar way, Christen et al. (2009) defined an entrainment rate for a unit flow velocity based on the heights and densities of the different bed layers (maximum of three layers); referring to this entrainment procedure as a *mass-controlled* model since the entrainment rate can be controlled directly. They found stress controlled procedures (i.e. velocity thresholds) to be somewhat artificial because the limit stress is arbitrarily chosen such that the measured entrainment rates are reached.

2.3. Numerical analyses

Some efforts have been made in the past to describe the entrainment process numerically and incorporate basal entrainment taking into account the shear stress of the erodible layer. We focus mainly on numerical analysis that define the process as entrainment rates and are embedded inside run-out models. Sassa (1998) proposed a model that takes into account the shearing at the bed channel induced by pore water pressure development. The pore water pressure is produced by undrained loading and if the undrained shear in the bed material is higher than the pore water pressure in the mixture a shear takes place. Therefore, a shear is dependant on the degree of saturation. De Joode and van Steijn (2003) used a similar approach based on water pore pressures development where the shear is dependent on the apparent friction angle of the bed material. One step further in this direction, Medina et al. (2008) proposed a static and a dynamic of approximation. In the static approximation the flow shear stress and the basal shear stress (based on the Mohr–Coulomb failure criterion) are calculated and the condition of equilibrium is calculated at each time step. If there is no equilibrium, the model calculates the magnitude of entrainment necessary to achieve equilibrium related to the erosion depth. This translates in a reduction of velocity because of the low quantity of momentum of the new mass. The dynamic approximation has the same principle of the flow and basal shear stress with the difference that the new mass is accelerated to the mean velocity of the flow, depending of the availability of momentum.

Sovilla et al. (2006) following up the approach proposed by Grigorian and Ostroumov in 1977 and based in her work on entrainment of snow avalanches, proposed a numerical model where the entrainment is localized at the head of the avalanche and step entrainment is not considered. The mass in flux rate is governed by mass and momentum conservation at the avalanche front but limited by mass availability. The model volumetric entrainment rate is given by an entrainment velocity that specifies the velocity at which the snow cover height is decreasing. This velocity is related to the applied pressure of the avalanche and the resisting strength of the snow cover. In an attempt to improve the mechanical and physical description of the process, Issler and Johannesson (2011) proposed adding an “entrainment force” term (equal to minus the entrainment rate times the mean flow velocity) in the momentum balance equations of depth-averaged gravity mass flow models. They found a relationship in the idealized setting of a quasi-stationary, entraining flow of a Bingham fluid, between the acceleration of the particles, entrainment rate and the velocity profile. It allows the velocity and stress profiles to be found in terms of entrainment rate. The latter can be determined by requiring that the bed shear stress be equal to the erosion threshold of the bed material. The deposition rate is limited by the difference between internal and bed shear stresses and by the inverse of the flow velocity. Mangeney et al. (2007b) described a partial fluidization model that takes into account the transition among sliding–flowing (Landau theory of phase transitions). The shear stress in a partially fluidized mass is composed of a dynamic part proportional to the shear strain rate and a static part independent of the strain. The magnitude of the static shear stress is controlled by the order parameter (liquid and solid phase) and the phase transition is controlled by the dynamic stresses and flow density. A fluidized layer may then develop at the bottom of a mass flow, and the flow sinks in the erodible bed and entrains the material. The model provides insights into the static/flowing transition within the granular mass and allows reproducing qualitatively granular flows over erodible bed when conventional depth-averaged model without entrainment fails. Iverson et al. (2011) stressed the importance of initial moisture content on entrainment and change in momentum and velocity of the flow. Based on measurements and mechanical considerations it was shown that entrainment of wet material results into an increase in velocity and flow momentum, while relative dry material show much less entrainment of mass and even a decrease in velocity. The main mechanism behind the scouring process is the generation of high pore pressures in the wetter material, resulting in a decrease in friction, which produces an increase in scouring of the bed surface. In their presented model, pore pressure generation plays also a critical role in the entrainment process and estimated the evolving local forces affecting momentum change during entrainment obtaining an expression for the net normalized force per unit basal area.

The work done in the past regarding the entrainment mechanism hints that the process plays an important role in the debris flow run-out evolution that leads to a better understanding of the flow behaviour. Currently, few dynamic run-out models include entrainment rates in their calculations. These rates can be classified based on the scheme used to estimate the amount of entrained material and the approach that defines and incorporates these rates into the dynamic models as: where the rate of entrained volume is defined or controlled directly by the user (mass controlled); and where the rate of entrained volume is estimated by the model by some particular limit stress (stress controlled). Difficulties still arise when trying to characterize the physics behind the entrainment phenomenon within dynamic models. A reason for this is that the introduction of entrainment in the models requires additional parameters, such as bed statigraphy, bed material and substrate strength which complicate practical calculations by introducing further uncertainties (Sovilla et al., 2007).

3. Model description

The model proposed here is based on earlier work of van Asch et al. in 2004. It is a dynamic one dimensional debris flow model that takes into account the entrainment concept based on the generation of excess pore water pressure through undrained loading of the in-situ material. The flow is treated as a laminar one phase, incompressible continuum material. Based on the Savage–Hutter model, the flow can be simulated by numerically solving the system of depth-averaged one-dimensional governing equations composed of the mass balance, momentum conservation equation, and the friction resistance based on the constitutive Coulomb–Bingham rheological equation (Coussot, 1997). Depth integration is based on the shallow water assumption, which applies where the length of the flowing mass is much greater than the thickness of the flowing mass. In these conditions the vertical velocity of the fluid is small, so that the vertical pressure gradient is nearly hydrostatic. This has become a classical approach for debris flow modeling (e.g. Pudasaini and Hutter, 2007; Hungr and McDougall, 2009; Christen et al. 2010). The flow is then modeled by a Saint–Venant type system derived in a reference frame linked to an inclined plane (Fig. 1) (Begueria et al., 2009). The mass (1) and momentum (2) can be described as follows:

$$\frac{\partial h}{\partial t} + c_x \frac{\partial (hu)}{\partial x} - \frac{\partial d_{sc}}{\partial t} = 0 \tag{1}$$

$$\frac{\partial u}{\partial t} + c_x u \frac{\partial u}{\partial x} = g c_x \left[g S_x - gK \frac{\partial c_x h}{\partial x} - g S_f - \frac{\partial u}{\partial t} \frac{\rho_s d_{sc}}{\rho h} \right] \tag{2}$$

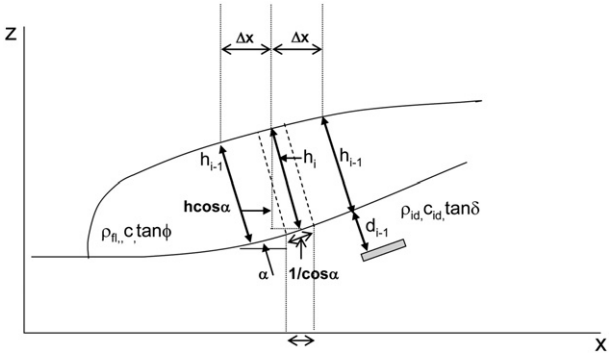

Fig. 1. Schematic force diagram for the simplified method of limiting equilibrium used in the model and representation of the model parameters. The numerical scheme is based on a perpendicular configuration referenced in a 2-D Euclidean space.

where, h is the flow height in the direction normal to the bed; u is the x component of the velocity, d_{sc} the scour depth; the coefficient $c_x = \cos\alpha_x$ is the direction cosine of the bed and α_x is the slope bed angle, which is taken positive when it dips downward in the (positive) x-direction. The momentum Eq. (2) is expressed in terms of acceleration (LT^{-2}). The second term on the left side of Eq. (2) represents the convective acceleration. The first term on the right side of Eq. (2) represents the acceleration due to gravity where S_x is the bed slope gradient. The second term on the right side is the pressure acceleration where K is the earth pressure coefficient, corresponding to the active and passive states in the Rankine's theory. K can have a value of 1 for a perfect fluid, but can vary greatly for plastic materials and ranges between two extreme values of the active and passive states: $K_a \leq 1 \leq K_p$ (Eq. (3)).

$$K_a = \frac{1 - sin\,\varphi}{1 + sin\,\varphi}$$
$$K_p = \frac{1 + sin\,\varphi}{1 - sin\,\varphi} \tag{3}$$

where φ is the internal friction angle of the mixture. The third term on the right side, S_f is the flow resistance due to frictional stress with the bed. The fourth and last term on the right side of the equation is the entrainment rate.

The resisting forces, S_f in Eq. (2), are dependant on the rheology of the material which controls the flow behavior and represents the bed shear stress of the flow. One-phase, depth-integrated models commonly assumes homogeneous and constant flow properties. A Coulomb–Bingham rheology model (Eq. (4)) is applied to determine a solution to the resisting force. The model assumes a linear stress–strain rate relationship once the yield strength is exceeded. Other types of rheologies can be integrated inside the model giving the possibility to simulate other types of flows and mass movements. For the purpose of this paper and the calibration of the 2003 Faucon event (clay-shale lithology with >10% clay in the grain size) a viscoplastic rheology was selected. Mud and debris flows have often been modeled as viscoplastic materials, i.e. as Bingham rheology with constant yield strength and viscosity (Begueria et al., 2009; Remaître, 2006). The Coulomb–Bingham rheology can be described as:

$$S_f = tan\varphi' + \frac{1}{\rho g h}\left(\frac{3}{2}\tau_c + \frac{3\eta}{h}u\right) \tag{4}$$

where, φ' is an apparent or basal of the flow friction angle, η is the dynamic viscosity (closely related to the percent concentration of solids) (kPa) and τc is a constant yield strength due to cohesion (kPa). Mangeney et al., 2007a, 2007b introduced a curvature radius, R_x, which describes local convexities or concavities in the slope profile and which influences the flow friction. The term gS_f in Eq. (2) has to be replaced as follows in Eq. (5) (see also Eq. (4)):

$$gS_f \Rightarrow \left(g - \frac{u^2}{R_x}\right) tan\varphi' + \frac{1}{\rho h}\left(\frac{3}{2}\tau_c + \frac{3\eta}{h}u\right) \tag{5}$$

where Eq. (6) (Mangeney et al., 2007a, 2007b):

$$\frac{1}{R_x} = \frac{\partial^2 b}{\partial x^2} \tag{6}$$

The internal pore fluid pressure is a transient property that is coupled to the normal stress and can dissipate during motion, making it extremely difficult to model (Begueria et al., 2009). Although some depth-averaged models have been developed that take into account the temporal evolution and spatial variation of pore fluid pressures (Iverson and Denlinger, 2001; Pitman and Le, 2005), in the presented model the pore pressure ratio (pore pressure/normal stress) is

assumed to be constant. This allows coupling the pressure dissipation into only one term, tanφ' (tangent of the apparent friction angle).

3.1. Numerical scheme

For the numerical implementation of hyperbolic partial differential equations such as Eqs. (1) and (2), we adopted a reasonably simple compromise solution as proposed by Begueria at al. (2009); that achieved a desired level of stability, accuracy and controlled diffusivity. It is convenient to write Eqs. (1) and (2) in a more compact vector notation, in order to describe the numerical solution which is used here in a 1D version:

$$\frac{\partial}{\partial t}(\mathbf{w}-\mathbf{r}) + \mathbf{k}_1\frac{\partial}{\partial_x}\mathbf{f} + \mathbf{k}_2(\mathbf{q}-\mathbf{s}) = 0$$

where

$$\mathbf{w} = \begin{pmatrix} h \\ u \end{pmatrix};\ \mathbf{r} = \begin{pmatrix} d_{sc} \\ 0 \end{pmatrix};\ \mathbf{k}_1 = \begin{pmatrix} c_x \\ uc_x \end{pmatrix};\ \mathbf{f} = \begin{pmatrix} hu \\ u \end{pmatrix};\ \mathbf{k}_2 = \begin{pmatrix} 0 \\ c_x \end{pmatrix};$$
$$\mathbf{q} = \begin{pmatrix} 0 \\ gS_x - K\dfrac{\partial(gc_x h)}{\partial x} \end{pmatrix};\ \mathbf{s} = \begin{pmatrix} 0 \\ gS_f + \dfrac{\partial u}{\partial t}\dfrac{\rho_s}{\rho}\dfrac{d_{sc}}{h} \end{pmatrix} \tag{7}$$

Begueria et al. (2009) implemented the model in an explicit finite difference (Eulerian) mesh, which in this 1D version means that the flow is described by variation in the conservative variables at points of fixed coordinates (i) as a function of time (n). Eq. (7) is solved numerically using a central difference forward scheme:

$$\mathbf{w_i^{n+1}} = W\left(\mathbf{w_i^n}\right) + \Delta t\left[\left(\mathbf{r_i^{n+1}} - \mathbf{r_i^n}\right) + \mathbf{k_{1i}^n}\left(\mathbf{f_{i+1}^n} - \mathbf{f_{i-1}^n}\right) + \mathbf{k_{2i}^n}\left(\mathbf{q_i^n} - \mathbf{s_i^{n+\frac{1}{2}}}\right)\right] \tag{8}$$

where Δt is the time step duration (s), and the pressure gradient term in $\mathbf{q}$ is computed by central differences. A common problem with such simple methods is the introduction of dispersive effects that lead to unphysical oscillations, especially in the presence of large gradients. Begueria et al. (2009) added a certain amount of numerical regularization, as introduced in Eq. (8) by the function $W(w^n{}_i)$:

$$W\left(\mathbf{w_i^n}\right) = (1-CFL)\mathbf{w_i^n} + CFL\frac{\mathbf{w_{i-1}^n} + w_{i+1}^{\mathbf{n}}}{2} \tag{9}$$

Eq. (9) performs a weighted spatial averaging over w, and the amount of numerical regularization is controlled by the value of the Courant–Levy–Friedrichs condition (CFL; see Eq. (10), below) at each point, so it is applied with preference to the areas of the flow that are experiencing sudden changes and have values of CFL typically in the range 0.5–1.

$$CFL = u\frac{\Delta t}{\Delta x}\sqrt{2} \tag{10}$$

Another problem with first-order time solutions is the over- and underestimation of the flow resistance term, which typically happens in accelerating and decelerating flows. To deal with this problem a two-step solution was adopted. Hence, the source term $s_i^{n+1/2}$ in Eq. (8) was evaluated at interleaved time steps to reduce over- and undershoots. The velocity components of w were estimated at times $n+1/2$ by applying Eq. (8) to w^n with $\Delta t = \Delta t/2$.

3.2. Entrainment rate scheme

Due to the limited knowledge of the physical processes that characterize the entrainment phenomenon, many dynamic run-out models include the entrainment process in a simplified way through calibration coefficients or entrainment rates that are pre-defined by the user. The methods available are based on empirical rules that estimate yield erosion rates. The main concept of these entrainment rate methods can be expressed as follows (Barbolini et al., 2005): –Erosion rate proportional to the flow velocity where the rates are a product of the velocity and an empirical coefficient that describes the flow properties (considering the density of the erodible bed and the flow). –Erosion rate proportional to the flow height where the erosion rate is considered a function of the flow load on the underlying bed cover. The rate is the product of the flow property coefficient and the minimum flow height that produces a load equal to the shear strength of the erodible bed. –Erosion rate growing with the square of the flow velocity where rate is the product of the flow property coefficient and a velocity threshold for erosion.

Entrainment of the bed material is the result of drag forces acting at the base of the flow, but may be aided by strength loss due to rapid undrained loading and liquefaction of the saturated channel. Rapid loading by the weight and momentum of the moving mass may cause failure and mobilization of these materials, which can have significantly different properties from the bulk of the moving material (McDougall and Hungr, 2005). Sassa (1998) stated the importance of knowing the pore pressure during the motion of the flow. He described three typical cases that cause pore pressure along the slip plane: 1) where the pore pressure at the slip plane is determined only by the pore pressure inside the landslide mass. The ground does not generate or dissipate pore pressure; 2) where the pore pressure at the slip plane is determined in the ground. Pore pressure caused by undrained loading and undrained shear inside the ground is so high in comparison with pore pressure inside the landslide mass that "shear" takes place in the ground; 3) where the higher pore pressure is inside the landslide mass and dissipates to the ground, so the pore pressure at the slip plane is affected by both the landslide mass and the ground. To implement the entrainment process in our model, it is assumed that the pore pressures are caused by the second case: the flow travels on the channel bed deposits causing an undrained loading process that generates a high-pore water pressure within the channel deposits and this helps to incorporate those deposits into the moving mass.

A loading of the bed deposits is generated when the moving mass flows on top. The model calculates this applied loading of the in-situ soil (Fig. 1) through the changes of vertical normal stress (Eq. (11)) and the shear strength (Eq. (12)) caused by the flow:

$$\Delta\sigma = p_{fl}gh\ cos^2\alpha \tag{11}$$

$$\Delta\tau = p_{fl}gh\ sin\alpha\ cos\alpha \tag{12}$$

where, ρ_{fl} is the density of the flow material, g is the gravity force, h the height of the flow and α the angle of the slope. Because of this loading, volume reduction and an increase in pore water pressure takes place. This increase in pore water pressure (Eq. (13)) is calculated based on the Skempton (1954) equation that expresses pore water pressures in an undrained triaxial test and modified by Sassa (1998) for an undrained direct shear test. Assuming that the soils along the shear zone inside the channel deposits are subjected to an undrained direct shear:

$$\Delta p = B_D(\Delta\sigma + A_D\Delta\tau) \tag{13}$$

where A_D and B_D are the pore pressure parameters in the direct shear state. Based on the laboratory tests of compressibility of the soils and assuming that the soils are not anisotropic, Sassa et al. (1985) proposed that the pore pressure parameter B_D is approximately the same with the B pore pressure parameter proposed by Skempton. B_D value is affected by the loaded stress level and its values are very

sensitive to the degree of saturation. In "saturated soil", the compressibility of the soil skeleton is almost infinitely greater than that of the pore water and essentially all of a stress increment applied to a saturated soil is carried by the pore fluid; $B_D = 1$. In "dry soil", the compressibility of the pore air is almost infinitely greater than the compressibility of the soil skeleton, and thus essentially all of the increment in total stress applied to the dry soil element is carried by the soil skeleton; $B_D = 0$. The transition of B_D values from a "saturated soil" to a "dry soil" is very drastic (e.g. values for a complete saturated state that ranges from 1 to 0.8 can quickly drop down to values of 0.1 or 0.2 for a slightly saturated soil). The pore pressure parameter A_D value changes with strain and probably the A_D value may increase after failure due to the crushing of grains, but dissipation of pore pressure may take place because shear zone is not as great as the compressed zone by the loaded normal stress. A value of A_D at failure can be assumed for the pore pressure parameter during motion. In general soft, loose soils have high values of A_D and the higher the shear strain the higher the value of A_D.

It is assumed that during an intense rain event, a ground water table may be formed in the surface bed layer. When there is ground water flowing perpendicular to the in situ soil, pore pressure (Eq. (14)) is calculated by:

$$P_{ini} = \rho_w g d_w \cos^2\alpha \tag{14}$$

The total pore water pressure is then (Eq. (15)):

$$p_{tot} = p_{ini} + \Delta p \tag{15}$$

New stresses at the bottom in-situ soil are then computed by (Eqs. 16 and 17):

$$\sigma_{tot} = \left(\rho_{fl} g h + \rho_{bot} g d\right) \cos^2\alpha \tag{16}$$

$$\tau_{tot} = \left(\rho_{fl} g h + \rho_{bot} g d\right) \sin\alpha \cos\alpha \tag{17}$$

where, ρ_{bot} is the density of the in-situ soil and d is the depth of the erodible layer. The factor of safety at the bottom (Eq. (18)) and top (Eq. (19)) of the in-situ soil is calculated as follows:

$$F_{bot} = \frac{c_{bot} + (\sigma_{tot} - p_{tot}) \tan\delta_{bot}}{\tau_{tot}} \tag{18}$$

$$F_{top} = \frac{c_{bot} + (\Delta\sigma - \Delta p) \tan\delta_{bot}}{\Delta\tau} \tag{19}$$

where, c_{bot} is the cohesion and δ_{bot} the friction angle of the in-situ soil. In the case where F_{top} and $F_{bot} < 1$ then d_{sc} which is the thickness of the failed layer equals the total thickness of the in-situ material (d). In the case where $F_{bot} < 1$ and $F_{top} > 1$, then d_{sc} is again the total thickness of in-situ material (d) and in the case where $F_{bot} > 1$ and $F_{top} < 1$, we have a portion of d which will fail and it is calculated as follows (Eq. (20)):

$$d_{sc} = \frac{1 - F_{top}}{F_{bot} - F_{top}} d \tag{20}$$

This computed failed mass is then incorporated to the flow enlarging its volume and changing its momentum.

High pore pressures in the presented model are generated by undrained loading and not by contraction of loose material during deformation of the bed by shearing (Iverson et al., 2011) Effective rise in pore pressure by loading occurs only, according to Skempton's law, when the material is at a degree of saturation of around 80% (Sassa, 1998), while in loose material as presented and measured by Iverson et al. (2011) an effective rise in pore pressure due to compaction occurs already when the soil is about halfway saturated.

4. Sensitivity analysis

A sensitivity analysis was performed to assess the impact of changes of the input parameters on the model outputs. This was conducted as a parametric study and was applied to the model to provide insight regarding the uncertainties in the output and where they can be allocated to the different sources of uncertainty in the model input. The objectives of the sensitivity analysis were: 1) to recognize which input parameters contribute the most to output variability; 2) which parameters are insignificant and can be held constant; and 3) to determine the optimal range within the parameter space for use in calibration studies.

The analysis was performed using the Bingham rheology on a synthetic profile (Fig. 2) and was divided in two parts based on the model structure: 1) sensitivity to the rheological parameters; and 2) sensitivity to the in-situ soil parameters that influences the scouring. The inputs of interest identified in the rheological model were: dynamic viscosity (η), earth pressure coefficient (K) and yield strength (τ strength). The input parameters selected for the in-situ soil were: friction angle (δ_{bot}), cohesion (c'_{bot}), density of the in-situ soil (ρ_{bot}), pore pressure parameter A_D, pore pressure parameter B_D and soil depth (h_{soil}).

All initial parameters were kept constant except the parameter chosen for the sensitivity (Table 1). All the inputs parameters except the pore pressure parameter B_D (in-situ soil) and the pressure parameter K (rheological model) were used with a variation of 10% from the initial simulation. For the pore pressure parameter B_D values ranging from 0 to 1 were chosen (saturation degree). The Rankine's active or passive pressure coefficient K (which depends on the velocity gradient downwards) was selected in this sensitivity analysis. The values are related to the internal friction angle, which we ranged from 1 to 0.10. The outputs selected to be measured were: 1) the velocity of the flow considered in relation with the time needed by the flow to reach the 120 m and 160 m cell (called "Time R"). These cells were selected in order to distinguish the velocity in the upper part and on the lower part of the profile; 2) the height of the flow for the cells 80 m, 100 m, 120 m, 140 m and 160 m at the time "Time R"; and 3) the mass balance measured at the "Time R".

The sensitivity was quantified as the percentage of change in the outputs subjected to a constant variation (percentage of change, in case of B_D: degree of saturation and in case of K: degree angle) in the input parameters. It was found out that the most sensitive rheological parameter was the dynamic viscosity (η). This parameter influences significantly the run-out distance and velocity of the flow however it does not play an important role in the entrainment process. Inside the model, increasing the dynamic viscosity decelerates the flow considerably. Confirming the retarding effect on the motion of the flow, an increase of 20% in the dynamic viscosity made the flow stop completely when the flow reached the gentler slope (Figs. 3 and 4).

The most sensitive in-situ soil parameters were the soil friction angle, the soil depth and the in-situ soil cohesion. They affect directly the amount of entrained material but do not have a substantial effect in the velocity of the flow. As the soil friction angle parameter increases, the entrained material by the flow in the steeper part of the slope augments until it reaches a threshold where the entrainment becomes continuous. But when the flow reaches the gentler slope, the increase of the friction angle had an opposite effect in the variation of mass (decreasing the entrained material). In contrast, the increase in the cohesion parameter enlarges the mass entrained until reaching a threshold of continuous entrainment both in the steep and gentle slope zones. The soil depth has a direct effect in the entrained material, an increment in the soil depth results in a growth of mass and entrainment (Figs. 3 and 4). This is in good agreement with the experimental observation made by Mangeney et al. (2010). The pore pressure parameter B_D has an influence on the variation of mass only when the in-situ soil starts to reach a complete degree of saturation of the soil with values of 0.8 to 1.

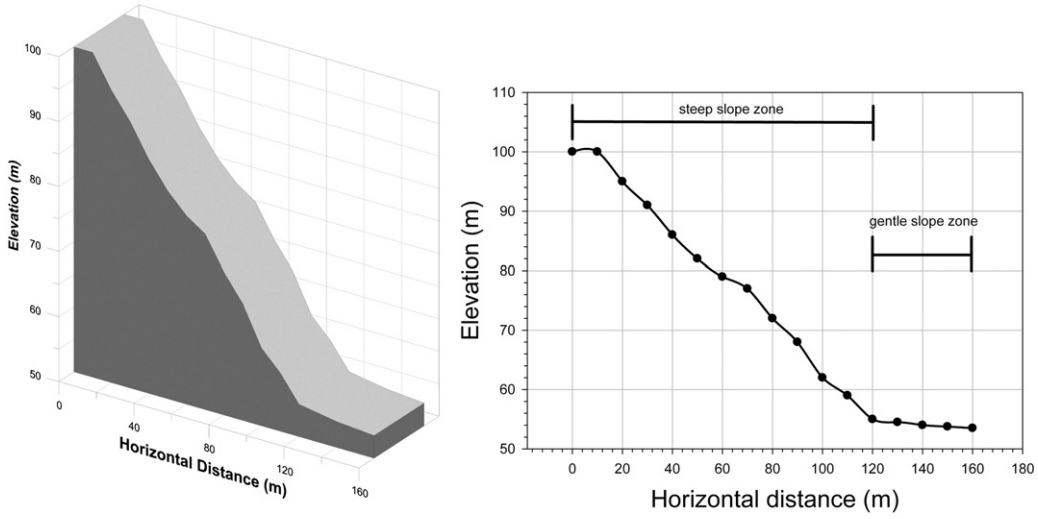

Fig. 2. Synthetic longitudinal profile used for the sensitivity analysis. The profile was divided into a steep slope zone and a gentle slope zone to assess the behavior of the flow with changing topography.

Table 1
Initial parameters used in the sensitivity analysis.

Debris Flow material (rheology)			In situ material (soil)					
T strength (kPa)	K pressure	ν (viscosity) (kPa/s)	δ_{bot} (°)	c_{bot} (kPa)	ρ_{bot} (kg/m^3)	A_D	B_D	h (soil) (m)
0.20	0.60	10.00	12	1	1600	0.6	0.1	0.3

5. Testing of model performance on observational data of the 2003 Faucon debris flow

The Faucon torrent (44°25′N, 6°40′E) is located on the south-facing slope of the Barcelonnette Basin (Southeast France). It has a catchment area of 8 km^2 and an altitude ranging from 1170 to 2982 m a.s.l. The higher parts of the massif consist of two sheet thrusts of faulted sandstones and calcareous sandstones. Slopes below this consist of Callovo–Oxfordian black marls, mainly composed of fragile plates and flakes packed in a clayey matrix. Most slopes are covered by various Quaternary deposits: thick taluses of poorly sorted debris; morainic deposits; screes and landslide debris. The incised channel has an average slope of about 20°, ranging from 80° in the headwater basin to 4° on the alluvial fan, and is approximately 5500 m in length (Remaître, 2006) (Fig. 5).

In recent times, the Faucon torrent has had two major events in 1996 and 2003. The 2003 event was considered to be modeled because of its significant overflowing in the alluvial fan area. The total volume of the debris flow in the source areas is estimated to be in the range from 7500 to 9500 m^3. Channel scouring is responsible for the difference between the 7500–9500 m^3 and the 60,000 m^3 that spread

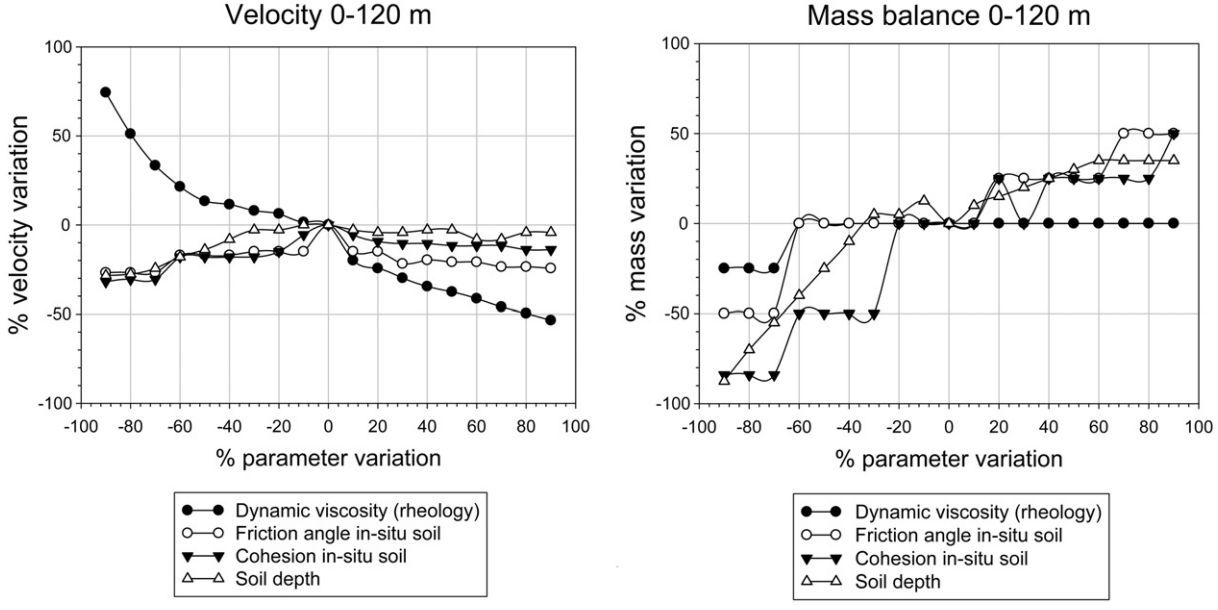

Fig. 3. Variation percentage of the velocity and the mass in regard to the percentage of change of the most sensitive parameters in the model during the steep slope section of the terrain path (0–120 m). The experimental tests of Iverson et al. (2011) show that uptake of wet material leads to an increase in speed, volume and momentum; while entrainment of relative dry material leads to lower velocities. In the presented model there is constant variation in speed and volume. To lower the speed for a dry material an increase in the viscosity must be considered.

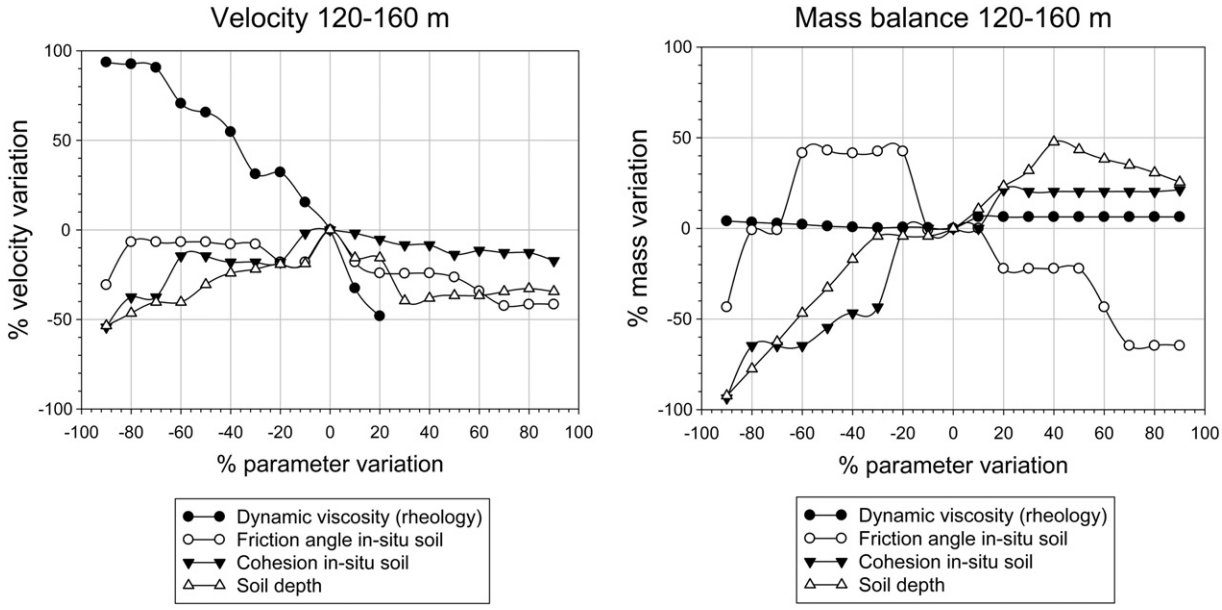

Fig. 4. Variation percentage of the velocity and the mass in regard to the percentage of change of the most sensitive parameters in the model during the gentler slope section of the terrain path (120–160 m).

over the fan (Remaître, 2006) (Fig. 6). The total length of the debris flow track is about 3500 m. Remaître et al. (2009) carried out a detailed post-event mapping of the erosion and deposits, the observations of the channel indicate that the scour depth ranges between 0.5 and 4 m. The channel scour rate per meter is calculated to 15 $m^3\ m^{-1}$. The velocities that were back calculated ranged from 6.4 to 8.9 ms^{-1} (Remaître, 2006).

The criteria chosen to compare the simulation results with the 2003 Faucon debris flow event were: 1) flow velocity; 2) deposit heights; and 3) run-out distance. The Faucon debris flow of 2003 has

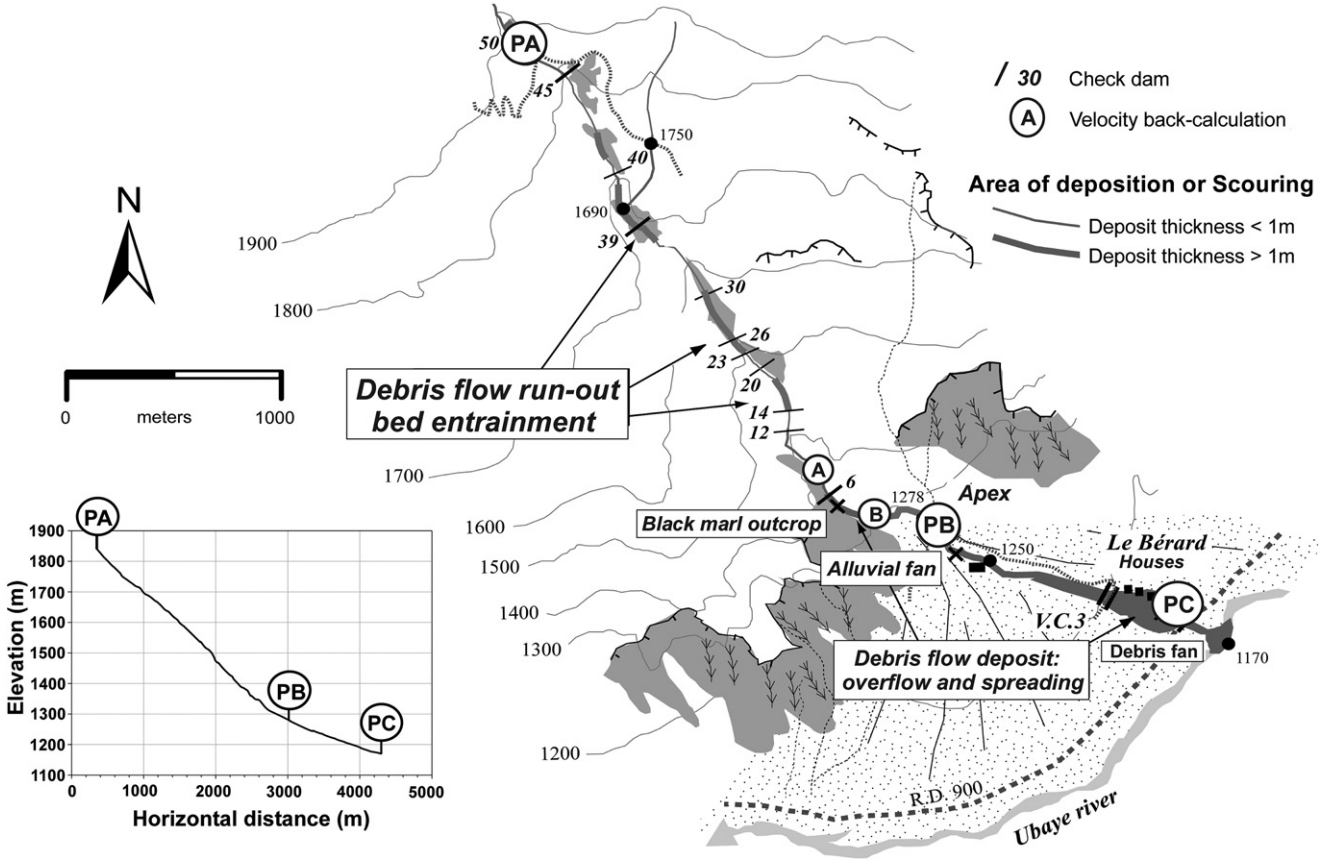

Fig. 5. Map and profile of the Faucon torrent (Remaître, 2006).

Fig. 6. Morphology of the eroded channel after the 2003 debris flow event at the Champerousse talus deposit in the upper part of the Faucon torrent.

already been modeled by Remaître et al. (2005a, 2005b) with a Bingham rheology with the BING 1D code (Imran, et al. 2001). The parameters for the best simulation were $\tau_y = 404$ Pa and $\eta = 122$ Pa s. The event has also been modeled based on Janbu's equilibrium method to calculate the yield strength and the shear stress which are then used in a simplified 2-parameter Bingham plastic rheology (Remaître 2006, Remaître et al. 2008). Other efforts to model the event in two dimensions and accounting for deposition in the fan were done by Begueria et al. (2009); they found that the best calibrated parameter sets were $\tau_y = 400$ Pa and $\eta = 67$ Pa s. with a Bingham rheology and $\tau_y = 200$ Pa, $\varphi' = 3.8^{\circ}$ and $\eta = 10$ Pa s. with a Coulomb-viscous rheology. However, these attempts did not considered the dynamic entrainment process that plays an important role in the development and behavior of the flow.

In our case, the calibration was completed through back analysis and was based on a trial and error adjustment of the input parameters defining the flow resistance and entrainment process. The inputs were adjusted until the computed criteria patterns matched as close as possible the real event. A profile of the torrent was created and the channel width of the torrent was considered for the volume estimation (Fig. 5). The initiation area was distributed in uniform columns of 10 m and the total released volume was 8443 m^3. A Bingham rheology was used to model the event. The parameters that best fitted the 2003 Faucon event were $\tau_y = 210$ Pa and $\eta = 63$ Pa s., which matches with a 52–53% of solids concentration by volume measured for the event (Remaître et al., 2008). A constant Rankine's earth pressure parameter of 1 assuming hydrostatic pressure and a density of the flow of 1850 kg m^{-3} were used for the simulation. The in-situ soil parameters found to match the entrainment amount of the event were $\varphi = 15^{\circ}$ and cohesion = 0.1 kPa. The density of the in-situ soil used was 1600 kg m^{-3}. The pore pressure parameter used were $A_D = 0.6$ and $B_D = 0.9$. These values correspond to an in-situ soil that has a high degree of saturation. The surface flow occurs in standard time and no air is entrapped under the water table. A homogeneous erodible in-situ soil depth of 3.5 m was found to be the value that agrees best with the quantity of entrained material by the original event. A calculation time step of 0.05 s was set up and the simulation had a time elapsed of 453.60 s.

The model predicted high velocities and higher amounts of entrainment when the slope is predominantly inclined and lower velocities and entrainment when it reaches the gentler slope in the lower section of the torrent. Fig. 7 shows the plots for maximum heights and velocities during the course of the flow. The final deposition volume is around 58338.91 m^3 (553% of increase in mass balance) with an average velocity during the whole event of 8.77 ms^{-1}. The application to the Faucon 2003 debris flow event give reasonable results in comparison to the field observations mainly based on the geometry of the deposits. Figs. 8 and 9 shows the relation between the flow height

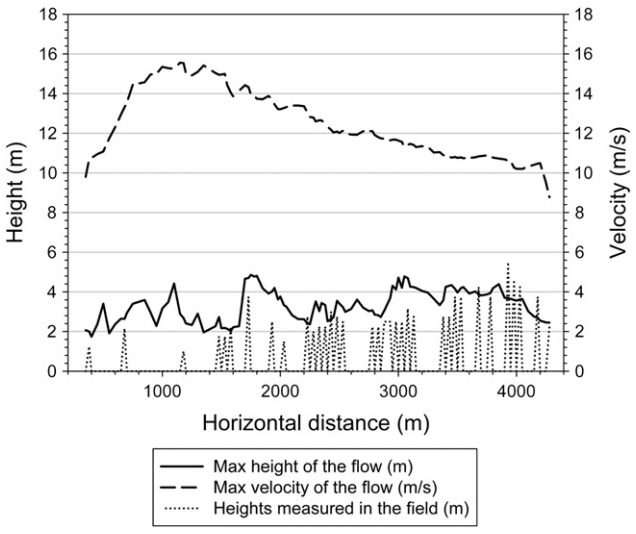

Fig. 7. Max velocity and max height of the flow during the flow course. The velocity distribution shows that the maximum velocity takes place when the debris is rushing down in the steepest part of the slope.

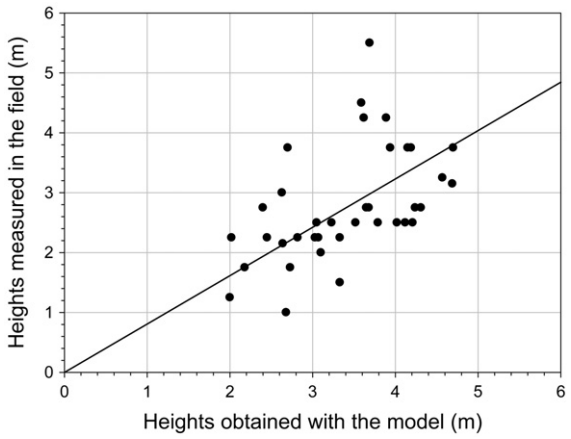

Fig. 8. Scatter plot between observed heights in the field after the event and the computed heights with a correlation coefficient of 0.808.

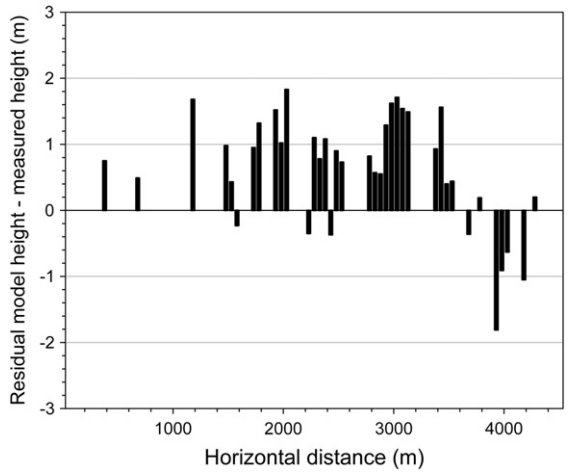

Fig. 9. Residuals values between the simulated and observed heights.

that the model predicts and the flow heights that were observed in the field. Relative higher deposits were simulated with an average height of approximately 3.23 m and a maximum height of 4.95 m. The difference between the heights and velocities calculated with the model and the real event measured in the field, can be explained by the fact that other processes are involved in the entrainment processes (i.e. abrasion) and due to the application of a 1D-model to a 3D-phenomenon. Fig. 10 shows the distribution of the entrained volume during the course of the flow and the accumulated final volume.

The model calculates the stability as a factor of safety of the in-situ soil based on the normal stresses, shear strength and increase of the pore pressure caused by the rapid loading of the flow in each time step. Once the stability threshold is exceeded, the entrainment process is dominated by the amount of soil capable to erode in the in-situ soil bed and the increasing variations of pore water pressures caused by the loading. This is in agreement with the numerical simulations of Mangeney et al., 2007b and experimental results obtained by Mangeney et al., 2010.

The increase of the pore water pressures is influenced by the loaded stress levels and its value changes with the degree of saturation. As a result and in accordance to the experimental results and theoretical predictions of Iverson et al., 2011; the in-situ soil becomes unstable and entrainment occurs (Fig. 11). Another important factor affecting the entrainment is the transition in the slope angle. The slope influences the variation of stresses on the in-situ soil and the behaviour of the flow during its course, explaining why entrainment is prominent on the steeper part of the track. The pore water pressures response is linked to the variation in the slope playing an important role in the entrainment process (Fig. 12). This agrees with the experimental results obtained from Mangeney et al. (2010) and Crosta et al. (2009) where they emphasize the importance of the slope inclination angle effect on the increase or decrease of the run-out distance.

To show the effects of introducing the entrainment process, a simulation was performed using the numerical model without entrainment. The maximum flow height along the flow path with and without entrainment is shown in Fig. 13. Entrainment has a significant influence on the flow depths and the run-out; the maximum flow heights and the distance travelled by the flow increase considerably with entrainment. The calculated maximum height of the flow without entrainment can be doubled or sometimes even tripled by the maximum heights estimated by taking into account the entrainment process; while the length of the run-out distance travelled can be increased by almost 1/3. This confirms the results obtained by Sovilla et al. (2007). Since the entrainment scheme presented here is influenced by the flow height, the addition

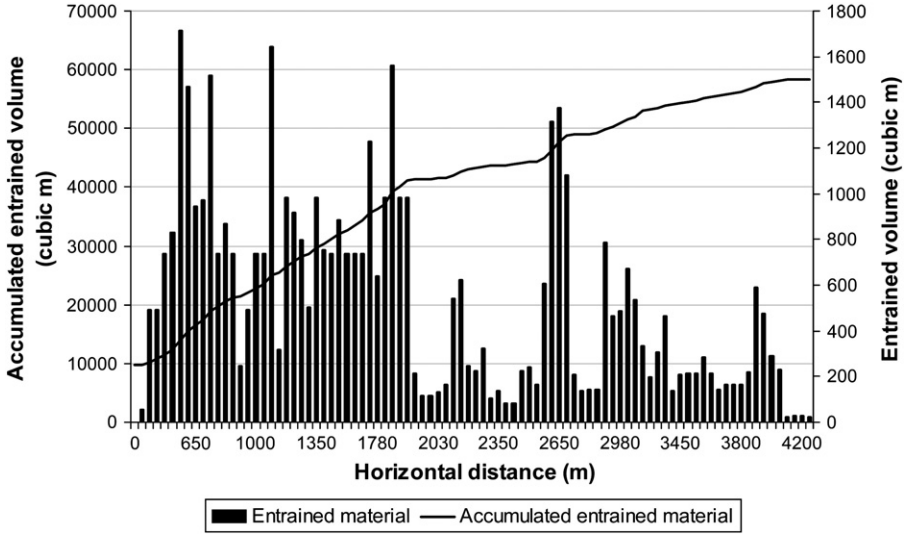

Fig. 10. Cumulative volumes of the deposits during the entrainment process and the entrained volume during the course of the flow.

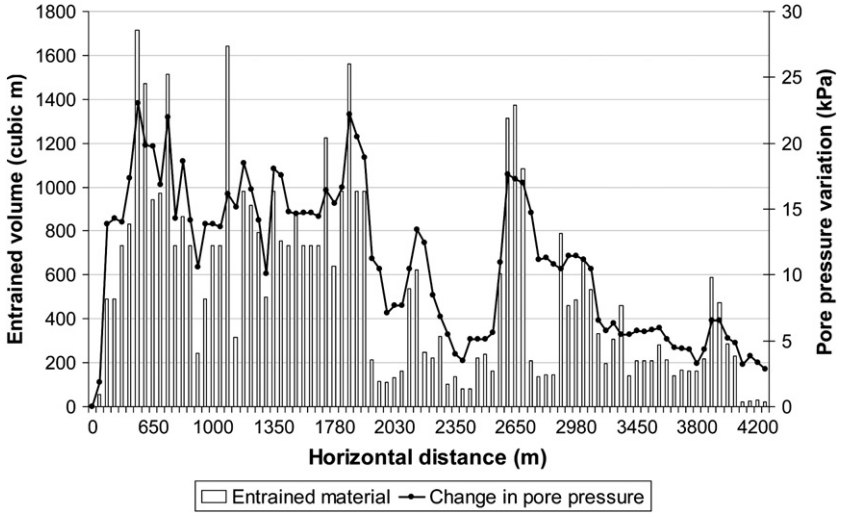

Fig. 11. Variation in pore pressure. The increase of the pore pressures produced by the undrained loading and undrained shear in the ground becomes high enough, that shear takes place in the in-situ soil causing this failed mass to be entrained by the flow.

of entrained material that results in bigger heights has a large effect on the overall behavior of the flow.

6. Discussion and conclusions

Entrainment is a key feature mechanism that is able to change significantly the mobility of the flow, the flow volume and its rheology. The model presented in this paper accounts for the entrainment process based on the generation of excess pore water pressure through undrained loading of the in-situ soil. The presented entrainment model highlights only one physical principle of entrainment which can be dominant during an event but other principles (as described before in this paper) might be valid and have a large effect on the overall behavior of the flow. A typical case where the model can be applied is when a soil mass has already failed because of a rainfall event (i.e. rise of groundwater table). At the same time, a high degree of saturation exists in some parts of the in-situ soil of the torrent or the channel. The failed mass moves progressively downstream, loading the saturated in-situ soil causing it to fail and enlarging of the flow volume. Further research is then needed to assess other dominant principles of entrainment under various conditions.

Based on a sensitivity test that was performed for the model, the rheological parameters and in particular the dynamic viscosity (η) influences the run-out distance and velocity but do not have a significant effect in the entrainment process. On the other hand the in-situ soil parameters such as the soil friction angle, the soil depth and cohesion affect directly the amount of entrained material. These parameters are directly linked with the strength of the in-situ soil and the amount of material to be entrained by the flow. The model calculates the stability of the in-situ soil based on a safety threshold. Once it is reached, the entrainment process is dominated by the amount of soil capable to erode and the fluctuations of the pore pressures caused by the loading.

A back-analysis of the Faucon 2003 debris flow and calibration of the model was carried out. The model estimates roughly the flow characteristics measured on the field (heights and velocity). Based on the results, a better estimation of the deposited volumes is an advantage of including entrainment in a model. However, a disadvantage of this is that no longer are the friction parameters

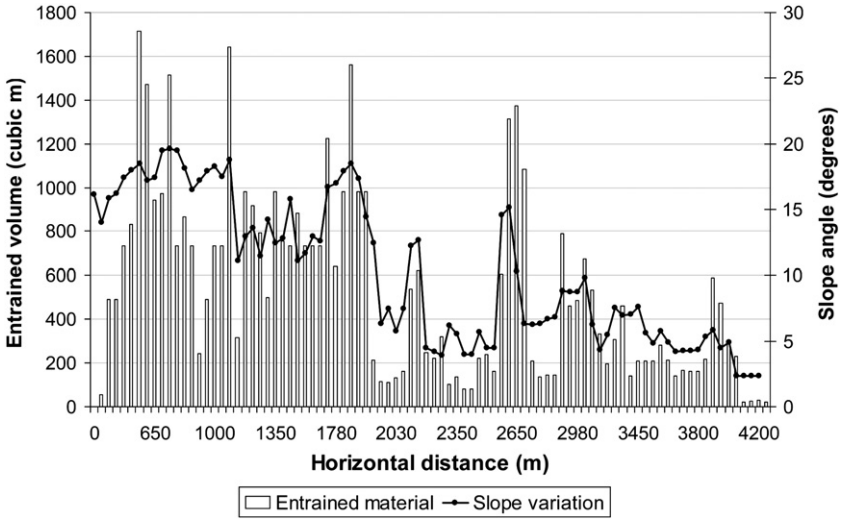

Fig. 12. Variation of the slope angle in the profile. The change in the slope angle influences the variation of stresses on the in situ soil by the loading and the behavior of the flow during its course.

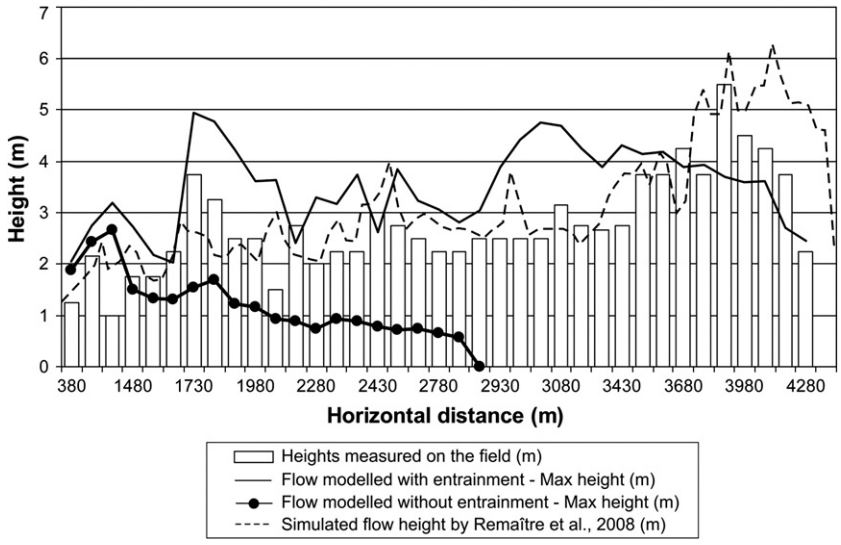

Fig. 13. Maximum heights along the flow path. Comparison between a simulation with and without entrainment. The modeled heights are compared to the heights measured on the field.

(rheological parameters) the only source of uncertainty but soils depths and pore pressure parameters.

We compared the results obtained with the model presented in this paper and the simulation done by Remaître et al. (2008) where he applied an entrainment rate proposed by Rickenmann et al. (2003). His results are also in good agreement with the past event; however slight differences can be observed between the two simulations when the flow reaches the gentler part of the slope. Although both models are strongly influenced by the slope gradient in the calculations of the entrainment, our proposed model is considerably sensitive with pronounced changes in the slope gradient.

Based on the importance of the entrainment process and its outcomes, research on debris flows and rapid mass movement dynamics can no longer disregard this phenomenon. Although, the process is not completely understood, the aforementioned simple model uses measurable geotechnical parameters in an attempt to describe the bulking phenomena of a real event. The model makes an effort to improve the application of numerical models that defines the dynamic behavior of debris flows which entrains large amounts of material. More and vast information of the process and an increase of the knowledge of the model parameters behavior are still needed to calibrate entrainment models in order to reduce the output uncertainty. Nevertheless, the results of this model hints that an entrainment model can lead to a better practice in the quantification of hazards.

Acknowledgments

This work has been supported by the Marie Curie Research and Training Network "Mountain Risks" funded by the European Commission (2007–2010, Contract MCRTN-35098). We thank the reviewers for their constructive and useful remarks. The authors would also like to thank Victor Jetten and Marcel Hurlimann for their comments and suggestions.

References

Barbolini, M., Biancardi, A., Cappabianca, F., Natale, L., Pagliardi, M., 2005. Laboratory study of erosion processes in snow avalanches. Cold Reg. Sci. Technol. 43, 1–9.

Begueria, S., van Asch, Th.W.J., Malet, J.-P., Grondahl, S., 2009. A GIS-based numerical model for simulating the kinematics of mud and debris flows over complex terrain. Nat. Hazards Earth Syst. Sci. 9, 1897–1909.

Bouchut, F., Fernandez-Nieto, E.D., Mangeney, A., Lagree, P.-Y., 2008. On new erosion models of Savage–Hutter type for avalanches. Acta Mech. 199, 181–208.

Chen, H., Lee, C.F., 2000. Numerical simulation of debris flows. Canadian Geotechnical J. 37, 146–160.

Chen, H., Crosta, G.B., Lee, C.F., 2006. Erosional effects on runout of fast landslides, debris flows and avalanches: a numerical investigation. Geotechnique 56 (5), 305–322.

Christen, M., Bartlett, P., Kowalski, J., Stoffel, L., 2009. Calculation of dense snow avalanches in three-dimensional terrain with the numerical simulation program RAMMS. RAMMS User manual.

Christen, M., Kowalski, J., Bartelt, P., 2010. RAMMS: numerical simulation of dense snow avalanches in three-dimensional terrain. Cold Reg. Sci. Technol. 63, 1–14.

Coussot, P., 1997. Mudflow Rheology and Dynamics. Balkema, Rotterdam.

Crosta, G.B., Imposimato, S., Roddeman, D., 2003. Numerical modelling of large landslides stability and runout. Nat. Hazards Earth Syst. Sci. 3 (6), 523–538.

Crosta, G.B., Imposimato, S., Roddeman, D., 2009. Numerical modelling of entrainment-deposition in rock and debris-avalanches. Engineering Geology 109 (1–2), 135–145.

De Joode, A., van Steijn, H., 2003. PROMOTOR-df: a GIS-based simulation model for debris flow hazard prediction. In: Rickenmann, D., Chen, C.L. (Eds.), "Debris-Flow Hazards Mitigation: Mechanics, Prediction, and Assessment," Proceedings 3rd International DFHM Conference, Davos, Switzerland, September 10–12, 2003. Millpress, Rotterdam, pp. 1173-1184.

Egashira, S., Honda, N., Itoh, T., 2001. Experimental study on the entrainment of bed material into debris flow. Phys. Chem. Earth C 26 (9), 645–650.

Gauer, P., Issler, D., 2004. Possible erosion mechanisms in snow avalanches. Annals Glaciology 38 (1), 384–392 (9).

Grigorian, S.S., Ostroumov, A.V., 1977. The Mathematical Model for Slope Processes of Avalanche Type (in Russian). Institute for Mechanics, Moscow State University, Moscow, Russia. scientific report, 1955.

Hungr, O., McDougall, S., 2009. Two numerical models for landslide dynamic analysis. Computers Geosciences 35, 978–992.

Hungr, O., Corominas, J., Eberhardt, E., 2005. Estimating landslide motion mechanism, travel distance and velocity. Proc. Int. Conf. on Landslide Risk Management, Vancouver, Canada. – Balkema, Leiden, pp. 99–128.

Imran, J., Harff, P., Parker, G., 2001. A numerical model of submarine debris-flow with graphical user interface. Computer Geosciences 27, 717–729.

Issler, D., Johannesson, T., 2011. Dynamical Consistency Constraints on Entrainment and Deposition in Depth-Averaged Models of Snow Avalanches and Other Gravity Mass Flows. Technical Note 20110112-00-1-TN. Norwegian Geotechnical Institute (NGI).

Iverson, R.M., Denlinger, R.P., 2001. Flow of variably fluidized granular masses across three-dimensional terrain. 1. Coulomb mixture theory. J. Geophysical Research 106, 537–552.

Iverson, R., Reid, M., Lahusen, R., 1997. Debris flow mobilization from landslides. Annu. Rev. Earth Planet. Sci. 25, 85–138.

Iverson, R.M., Reid, M.E., Logan, M., LaHausen, R.G., Godt, J.W., Griswold, J.P., 2011. Positive feedback and momentum growth during debris-flow entrainment of wet bed sediment. Nature Geoscience 4, 116–121.

Malet, J.-P., Remaître, A., Maquaire, O., 2004. Runout modeling and extension of the threatened area associated with muddy debris flows. Geomorphologie relief processus environnement 3, 195–210.

Mangeney, A., Bouchut, F., Thomas, N., Vilotte, J.P., Bristeau, M.O., 2007a. Numerical modeling of self-channeling granular flows and of their levee-channel deposits. J. Geophysical Research 112, F02017. doi:10.1029/2006JF000469.

Mangeney, A., Tsimring, L.S., Volfson, D., Aranson, I.S., Bouchut, F., 2007b. Avalanche mobility induced by the presence of an erodible bed and associated entrainment. Geophysical Research Letters 34, L22401. doi:10.1029/2007GL031348.

Mangeney, A., Roche, O., Hungr, O., Mangold, N., Faccanoni, G., Lucas, A., 2010. Erosion and mobility in granular collapse over sloping beds. J. Geophysical Research 115, F03040. doi:10.1029/2009JF001462.

Mangeney-Castelnau, A., Bouchut, F., Vilotte, J.P., Lajeunesse, E., Aubertin, A., Pirulli, M., 2005. On the use of Saint–Venant equations for simulating the spreading of a granular mass. J. Geophys. Res. 110, B09103. doi:10.1029/2004JB003161.
McDougall, S., Hungr, O., 2005. Dynamic modelling of entrainment in rapid landslides. Can. Geotech. J. 42, 1437–1448.
Medina, V., Hürlimann, M., Bateman, A., 2008. Application of FLATModel, a 2D finite volume code, to debris flows in the northeastern part of the Iberian Peninsula. Landslides 5, 127–142.
Naef, D., Rickenmann, D., Rutschmann, P., McArdell, B.W., 2006. Comparison of flow resistance relations for debris flows using a one-dimensional finite element simulation model. Nat. Hazards Earth Syst. Sci. 6, 155–165.
O'Brien, J.S., Julien, P.Y., Fullerton, W.T., 1993. Two-dimensional water flood and mudflow simulation. J. Hydrol. Eng. 119 (2), 244–261.
Papa, M., Egashira, S., Itoh, T., 2004. Critical conditions of bed sediment entrainment due to debris flow. Nat. Hazards Earth Syst. Sci. 4, 469–474.
Pastor, M., Haddad, B., Sorbino, G., Cuomo, S., Drempetic, V., 2009. A depth-intergrated, coupled SPH model for flow-like landslides and related phenomena. Int. J. Numer. Anal. Meth. Geomech. 33, 143–172.
Pirulli, M., Mangeney, A., 2008. Results of back-analysis of the propagation of rock avalanches as a function of the assumed rheology. Rock Mechanics Rock Engineering 41 (1), 59–84.
Pitman, B.E., Le, L., 2005. A two-fluid model for avalanche and debris flow. Phil. Trans. R. Soc. A. 363, 1573–1601.
Pouliquen, O., Forterre, Y., 2002. Friction law for dense granular flows: application to the motion of a mass down a rough inclined plane. J. Fluid Mechanics 453, 133–151.
Pudasaini, S.P., Hutter, K., 2007. Avalanche dynamics—dynamics of rapid flows of dense granular avalanches. Springer – Verlag, Berlin.
Remaître, A., 2006. Morphologie et dynamique des laves torrentielles: Applications aux torrents des Terres Noires du bassin de Barcelonnette (Alpes du Sud). Ph.D. thesis.
Remaître, A., Malet, J.-P., Maquaire, O., 2005a. Morphology and sedimentology of a complex debris flow in a clay-shale basin. Earth Surf. Process. Landforms 30, 339–348.
Remaître, A., Malet, J.-P., Maquaire, O., Ancey, C., Locat, J., 2005b. Flow behaviour and runout nodelling of complex debris flow in a clay-shale basin. Earth Surf. Process. Landforms 30, 479–488.
Remaître, A., van Asch, Th.W.J., Malet, J.-P., Maquaire, O., 2008. Influence of check dams on debris flow run-out intensity. Nat. Hazards Earth Syst. Sci. 8, 1403–1416.
Remaître, A., Malet, J.-P., Maquaire, O., 2009. Sediment budget and morphology of the 2003 Faucon debris flow (South French Alps): scouring and channel-shaping processes. Proc. Landslide Processes: from geomorphological mapping to dynamic modelling, pp. 75–80.
Rickenmann, D., Weber, D., Stepanov, B., 2003. Erosion by debris flows in field and laboratory experiments. In: Rickenmann, D., Chen, C.L. (Eds.), "Debris-Flow Hazards Mitigation: Mechanics, Prediction, and Assessment," Proceedings 3rd International DFHM Conference, Davos, Switzerland, September 10–12, 2003. Millpress, Rotterdam, pp. 883–894.
Sassa, K., 1998. Geotechnical model for the motion of landslides. Proc. Vth ISL, Lausanne, pp. 37–55.
Sassa, K., Kaibori, M., Kitera, N., 1985. Liquefaction and undrained shear of torrent deposits as the cause of debris flows. Proc. Inter. Symp. On Erosion, Debris flows and Disas. Prev, pp. 231–236.
Savage, S.B., Hutter, K., 1989. The motion of a finite mass of granular material down a rough incline. J. Fluid Mechanics 199, 177–215.
Skempton, A.W., 1954. The pore-pressure coefficients A and B. Geotechnique 4, 143–147.
Sovilla, B., Burlando, P., Bartlet, P., 2006. Field experiments and numerical modeling of mass entrainment in snow avalanches. J. Geophys. Res. 111, F03007. doi:10.1029/2005JF000391.
Sovilla, B., Margreth, S., Bartelt, P., 2007. On snow entrainment in avalanche dynamics calculations. Cold Reg. Sci. Technol. 47, 69–79.
Takahashi, T., 1978. Mechanical characteristics of debris flows. J. Hydraulics Division ASCE 104, 1153–1169 (HY8).
Takahashi, T., 2001. Mechanics and simulation of snow avalanches, pyroclastic flows and debris flows. Spec. Publs. Int. Ass. Sediment. 31, 11–43.
Takahashi, T., 2009. A review of Japanese debris flow research. International J. Erosion Control Engineering. 2 (1).
Van Asch, Th.W.J., Malet, J.-P., van Beek, L.P.H., Amitrano, D., 2007. Techniques, issues and advances in numerical modelling of landslide hazard. Bull. Soc. géol. Fr. 178 (2), 65–88.
Van Westen, C.J., van Asch, Th.W.J., Soeters, R., 2006. Landslide hazard and risk zonation—why is it still so difficult? Bull Eng Geol Env. 65, 167–184.
Vandine, D.F., Bovis, M., 2002. History and goals of Canadian debris-flow research, a review. Natural Hazards 26, 69–82.
Voellmy, A., 1955. Uber die Zerstorunskraft von Lawinen (On breaking force of avalanches). Schweizerische Bauzeitung 73, 212–285.